

From the power law to extreme value mixture distributions

Clement Lee¹ and Emma Eastoe¹

¹Department of Mathematics and Statistics, Lancaster University,
UK

December 22, 2024

Abstract

The power law is useful in describing count phenomena such as network degrees and word frequencies. With a single parameter, it captures the main feature that the frequencies are linear on the log-log scale. Nevertheless, there have been criticisms of the power law, and various approaches have been proposed to resolve issues such as selecting the required threshold and quantifying the uncertainty around it, and to test hypotheses on whether the data could have come from the power law. As extreme value theory generalises the (continuous) power law, it is natural to consider the former as a solution to these problems around the latter. In this paper, we propose two extreme value mixture distributions, in one of which the power law is incorporated, without the need of pre-specifying the threshold. The proposed distributions are shown to fit the data well, quantify the threshold uncertainty in a natural way, and satisfactorily answer whether the power law is useful enough.

Keywords: Power law; Extreme value theory; Degree distribution; Mixture distribution; Threshold uncertainty

Correspondence: clement.lee@lancaster.ac.uk

1 Introduction

The power law is a principle in which the ratio of the relative change in two quantities is (approximately) constant. In the context of statistics and data analysis, this means the relative change in the size of the quantity of interest is proportional to the relative change in the frequency. The power law has been applied to data in various fields and topics, such as astrophysics (Jóhannesson

et al., 2006), quantitative linguistics (Montemurro, 2001, Bell et al., 2012), casualty numbers (Bohorquez et al., 2009, Friedman, 2015, Gillespie, 2017), and city sizes by Newman (2005) and Clauset et al. (2009), who both provided numerous examples of power law applications.

One particular class of discrete data for which the power law is often suitable is the degree distribution or related characteristics of *networks*. Examples include networks of links on the World-Wide Web (Barabási and Albert, 1999, Albert et al., 1999, Faloutsos et al., 1999), social networks (Lee, 2014, Lee and Oh, 2014, Varga, 2015), coauthorship/collaboration and citation networks (de Solla Price, 1976, Newman, 2001a,b, 2004, Thelwall and Wilson, 2014, Ji and Jin, 2016, Arroyo-Machado et al., 2020), retweet counts Bhamidi et al. (2015), Mathews et al. (2017). As an example, consider the citation network of a computer science conference, which corresponds to the top-right plots of Figures 1 and 2, and has been analysed by Lee et al. (2019). Another type of network is one summarising software dependencies, which have been studied in conjunction with the power law by, for example, LaBelle and Wallingford (2004), Baxter et al. (2006), Jenkins and Kirk (2007), Wu et al. (2007), Louridas et al. (2008), Zheng et al. (2008), Kohring (2009), Li et al. (2013), Bavota et al. (2015), Cox et al. (2015). In this paper we consider the package dependencies in the Comprehensive R Archive Network (CRAN), plotted in the bottom-right of Figures 1 and 2. Both the data set and the programming functions for the analysis in this paper are available in the R package **crandep** (Lee, 2020).

Networks with in-degree distributions which follow the power law are called scale-free networks. Note that as the in-degrees of the nodes are usually of greater interest than the out-degrees are, we refer to the former hereafter whenever the degree distribution is mentioned. One reason for applying the power law to seemingly scale-free networks is the potential of *generative* models that result in the degree distribution following the power law. Such models are useful descriptions of how the nodes in the network connect with each other according to some simple rules, and can be used for simulating networks in order to study their behaviour. Among the numerous models that have been proposed as the generating mechanism of scale-free networks, the most prominent is the preferential attachment model by (Barabási and Albert, 1999), which originated from the cumulative advantage process by de Solla Price (1976). Studies on the extensions of the preferential attachment model, and whether they will result in a power law degree distribution, include Albert et al. (2000), Krapivsky and Redner (2001), Krapivsky et al. (2001), Vázquez et al. (2002), Bollobás et al. (2003), Wang and Chen (2003), Ramasco et al. (2004), Noh et al. (2005), Hsiao et al. (2007), Li et al. (2013), Bhamidi et al. (2015), and Sheridan and Onodera (2018). While the generating mechanism is not the focus of this paper, the influential and pioneering papers of Barabási and Albert (1999), Albert et al. (1999), Newman (2005) and Clauset et al. (2009) are embodiment of preferential attachment.

The natural way of modelling data that seems to follow the power law, network related or not, is through the Pareto distribution. Specifically, a positive continuous random variable Z follows the Pareto distribution if its probability

density function (PDF) is

$$f_Z(z) = \begin{cases} \frac{(\alpha-1)}{u} \left(\frac{z}{u}\right)^{-\alpha}, & z > u, \\ 0, & \text{otherwise,} \end{cases} \quad (1)$$

where $u > 0$ is a threshold, and the parameter $\alpha > 1$ is often known as the exponent in the literature. The Pareto distribution and the *continuous* power law are synonymous hereafter. However, as many data for which the power law seems appropriate are discrete, it is natural to consider the discrete counterpart. Specifically, a discrete random variable X follows the discrete power law if its probability mass function (PMF) is

$$p_X(x) = \begin{cases} \frac{x^{-\alpha}}{\zeta(\alpha, u)} & x = u, u+1, \dots \\ 0 & \text{otherwise,} \end{cases} \quad (2)$$

where

$$\zeta(\alpha, k) = \sum_{i=k}^{\infty} i^{-\alpha} = \sum_{i=0}^{\infty} (k+i)^{-\alpha}$$

is the Hurwitz zeta function, and u is a positive integer. The discrete power law distribution is sometimes called the zeta distribution. Related but not equivalent to the discrete power law is the Zipf's law or its generalisation the Zipf-Mandelbrot law, which is commonly used for rank data in quantitative linguistics (Montemurro, 2001, for example). However, we will focus on the Pareto distribution and the discrete power law in this paper, because of their wide-spread use and of the relationship of the former with our proposed distributions, to be explained in Sections 2 and 3.

When it comes to modelling real-life data, an indication that the power law may be appropriate is that on the log-log scale the empirical frequencies (or histograms) display an approximately linear relationship with the data values. This is because, according to Equation 1, the Pareto distribution implies that $\log f_Z(z)$ is linear with $\log z$ with slope $-\alpha$. An equivalent result holds for the discrete power law. A similar diagnostic is checking linearity of the empirical survival function on the same scale. This is because, for the Pareto distribution,

$$S_Z(z) := \Pr(Z > z) = \left(\frac{z}{u}\right)^{-(\alpha-1)} \quad (3)$$

for $z > u$, meaning that its survival function is a straight line with slope $1-\alpha$ on the log-log scale. Such approximate linearity on the log-log scale is observed in Figures 1 and 2, which show the frequency and survival functions, respectively, for a range of examples. In all cases, both functions are shown on the log-log scale. Among these examples, "Native Americans" and "US Americans" are casualty numbers in armed conflicts and have been analysed by Bohorquez et al. (2009), Friedman (2015) and Gillespie (2017), while "Swiss-Prot" and "Moby Dick" are data sets of word frequencies investigated by Bell et al. (2012) and Newman (2005), respectively. These four data sets are available in the R

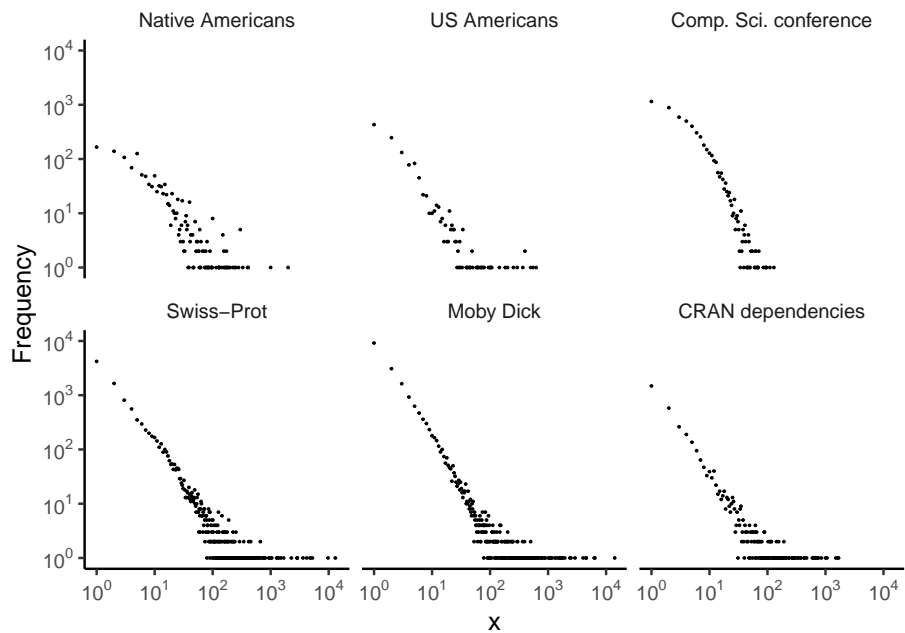


Figure 1: Frequency plots for six different data sets on log-log scale.

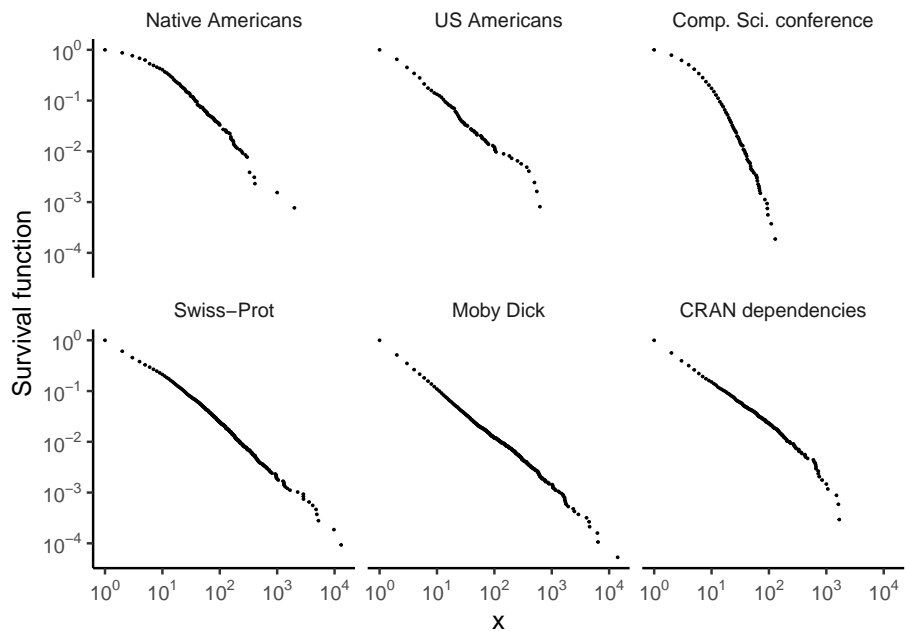


Figure 2: Survival function for six different data sets on log-log scale.

package **poweRlaw** (Gillespie, 2015), and the last data set is also available in the Python package **powerlaw** (Alstott et al., 2014).

Whilst the plots for all six data sets are approximately linear, this approximation is questionable, in particular for the first row to fit the discrete power law and describe each data set with just one parameter. However, the data is not entirely linear in some cases, as seen in the first row of Figures 1 and 2, at best partially or piecewise linear, as the left “tail” shows different behaviour to the right tail. Therefore, it is more appropriate to fit the power law to a subset of the data. As the large data values are usually of greater interest, the common approach is to apply the power law to data above a threshold u , hence the suitability of the Pareto distribution or the discrete power law. However, the choice of u has to be made prior to fitting the power law, and is therefore user-subjective. Such subjectivity will have an impact on how representative the results are, as different thresholds could lead to different estimates of α . Furthermore, as the subset of data to be fitted is dependent on u , the likelihoods obtained under different thresholds correspond to different subsets of the full data set, making it difficult to treat u as a parameter and carry out inference by, for example, maximising the profile likelihood of u .

Clauset et al. (2009) provided an approach to selecting u through the use of the Kolmogorov-Smirnov statistic. The power law is fitted to a range of thresholds, and the threshold that minimises the maximum distance between the empirical and fitted CDFs is selected. They also provided procedures for quantifying the threshold uncertainty through bootstrap, as well as hypothesis tests for whether the power law is plausible for the data. These procedures are available in the R package **poweRlaw** (Gillespie, 2015). Related to them is Corral et al. (2012) who provided a practical recipe to fit discrete power law. These approaches are useful but require additional procedures after fitting the power law. Furthermore, the issue with the loss of information is yet to be resolved.

Apart from the threshold selection problem, some have argued that the power law is inadequate for network degree distributions, and that scale-free networks are not without disadvantages. Stumpf et al. (2005) found that sampling from scale-free networks does not result in (smaller) scale-free networks. Stumpf and Porter (2012) questioned the ubiquity of the power law in different disciplines. Bessi (2015) provided a two samples test for discrete power law. Mohd-Zaid (2016) proposed two statistical tests for testing if a network is a preferential attachment one. Broido and Clauset (2019) found that scale-free networks are rare in reality, and for most networks the log-normal distribution is sufficient for the data. That the log-normal distribution is an adequate alternative has been examined and supported by, for example, Thelwall and Wilson (2014), Sheridan and Onodera (2018), and Arroyo-Machado et al. (2020). The implication of the inadequacy of the power law is that the preferential attachment model, or any model that leads to power law degree distributions, might be inadequate for the generating mechanism of the network. Therefore, an adequate and correctly specified degree distribution is the key to the development of more realistic generative network models.

In this paper we aim at developing probability distributions that can fit well to degree distributions as well as other kinds of data that have been suggested to arise from the power law. In particular, an improved fit for the larger values can be achieved by the use of extreme value theory, which has been developed precisely for studying the distribution of the largest or smallest values in a sample. In fact, one commonly used distribution in extreme value theory is the generalised Pareto distribution (GPD), which, as its name suggests, is a generalisation of the continuous power law. While extrapolation using the GPD is possible, our focus is on a best fitting distribution to describe the within-sample behaviour. Another reason for the use of extreme value theory is that threshold selection and uncertainty can be addressed through the use of extreme value mixture distribution (Scarrott and MacDonald, 2012, for example), in which the GPD is a component.

The rest of this paper is divided as follows. The GPD is introduced in Section 2, with the focus on its connection with the Pareto distribution. The approaches to threshold selection in extreme value theory, both with and without the use of mixture distributions, will also be mentioned. The proposed distributions are introduced in Section 3, with their corresponding likelihoods derived. The inference approach and algorithm are detailed in Section 4. Applications of the mixture distributions to the six sets of data we have seen are presented in Section 5. Section 6 concludes the paper.

2 Extreme value theory

We start by introducing the generalised Pareto distribution (GPD) and showing the connection between this and the continuous power law. Also introduced is one approach to dealing with threshold selection, in which the GPD is incorporated in mixture distributions.

The PDF of the GPD is

$$g(z) = \begin{cases} \frac{1}{\sigma_0} \left[1 + \xi \frac{z - \mu}{\sigma_0} \right]_+^{-1/\xi-1}, & \xi \neq 0, \\ \frac{1}{\sigma_0} \exp \left[-\frac{z - \mu}{\sigma_0} \right], & \xi = 0, \end{cases} \quad (4)$$

where $A_+ := \max\{A, 0\}$, μ is the location parameter, $\sigma_0 > 0$ is the scale parameter, and ξ is the shape parameter. There is no loss in generality in working primarily with the upper expression as taking its limit as $\xi \rightarrow 0$ yields the lower expression. Now, if a random variable Z follows exactly the GPD, its distribution *conditional on* $Z > u$ will have the density

$$g_u(z) = \frac{1}{\sigma_0 + \xi(u - \mu)} \left[1 + \frac{\xi(z - u)}{\sigma_0 + \xi(u - \mu)} \right]_+^{-1/\xi-1}. \quad (5)$$

The GPD can be shown to be a generalisation of the continuous power law in

the case of $\xi > 0$ and $\sigma_0 = \xi\mu$, where Equation 5 becomes

$$g_u(z) = \frac{1}{\xi u} \left(\frac{z}{u} \right)^{-(1/\xi+1)}, \quad (6)$$

which is the density in Equation 1 with $\alpha = 1/\xi + 1$. The condition $\xi > 0$ is equivalent to $\alpha > 1$ in the continuous power law.

The above result is exact only if Z follows the GPD. However, Pickands (1975) showed that the GPD approximates the conditional tail $\Pr(Z > z|Z > u)$ of an arbitrary CDF F , provided that u is sufficiently high. This approximation follows from asymptotic results which state that the above conditional distribution Equation 5 holds exactly in the limit as $u \rightarrow \infty$, for almost all continuous distributions F . In the context of data analysis, this motivates the use of the GPD as a model for the observations above a high threshold. In practice, for identifiability, the GPD in Equation 5 can be re-parametrised as (ϕ_u, σ, ξ) where $\phi_u := \Pr(Z > u) = \left[1 + \xi \frac{u-\mu}{\sigma_0} \right]_+^{-1/\xi}$ is the exceedance probability, and $\sigma = \sigma_0 - \xi\mu$. This parametrisation will be used hereafter. For other practical considerations, see, for example, Coles (2001).

As the GPD generalises the continuous power law, it seems natural to apply the former to data for which the latter is useful but possibly inadequate. A recent example is Wan et al. (2020), who applied the preferential attachment model by Krapivsky and Redner (2001) and Bollobás et al. (2003) to both in- and out-degree distributions, and examined the parameter estimation under data corruption or model misspecification. They found that the semi-parametric estimator (Hill, 1975) of ξ is more robust than its maximum likelihood estimator. The threshold is selected according to the procedure by Clauset et al. (2009) outlined in Section 1. Related is the R package **ptsuite** (Munasinghe et al., 2019), which provided functions for both estimators of ξ alongside other estimators, albeit with no automated procedure for selecting u . Our approach is different from Wan et al. (2020) in that the proposed distributions are fully parametric, and that the procedure of threshold selection is not required as u is treated as a parameter of the distributions.

2.1 Threshold selection and mixture distributions

That the threshold u has to be specified before fitting the GPD is the same as in fitting the power law, discrete or continuous. For the former, specification is aided by fitting the GPD over a range of values, and looking the plots of the maximum likelihood estimates (MLEs) of σ and ξ . The threshold to be chosen is then the one above which the parameter estimates look stable, with their uncertainty taken into account. While this diagnostic approach is illustrated by Coles (2001) is useful, a subjective decision is still required, while the uncertainty around the threshold is not accounted for. One solution to the problem of threshold selection and uncertainty is the use of mixture distributions. Examples include Frigessi et al. (2002), Behrens et al. (2004), Tancredi et al. (2006), Carreau and Bengio (2009), Zhao et al. (2010), MacDonald et al. (2011), do

Nascimento et al. (2012), and So and Chan (2014). A comprehensive review is provided by Scarrott and MacDonald (2012), and an R package **evmix** is provided by Hu and Scarrott (2018).

The principle of an extreme value mixture distribution is to assume a GPD for the observations above u and some other distribution H for those below u , while allowing u to vary as a parameter and therefore be estimated. Specifically, assuming Y is a positive continuous random variable with density function $h(\cdot)$ and CDF $H(\cdot)$, we consider another positive random variable Z which equals Y if $Z \leq u$, where u is a positive threshold. Conditional on $Z > u$, Z follows the GPD with scale parameter σ and shape parameter ξ_2 . The density function of this mixture distribution for Z is

$$f_Z(z) = \begin{cases} (1 - \phi_u) \times \frac{h(z)}{H(u)}, & z \leq u, \\ \phi_u \times g_u(z), & z > u. \end{cases} \quad (7)$$

The parameters are suppressed throughout for notational simplicity, and $h(\cdot)$ and $g_u(\cdot)$ will be referred to as the bulk and tail distributions, respectively. Both ϕ_u and $H(z)$ are required for f_Z to be a proper density i.e. to integrate to 1. According to the threshold stability for the GPD, we can write $\sigma_u = \sigma + \xi_2 u$, with $\sigma (> 0)$ independent of u . When $\xi_2 = 0$, the lower expression becomes $\phi_u \times \exp(-\frac{z-u}{\sigma})$, which is the limit of the original expression as $\xi_2 \rightarrow 0$. We give an example mixture distribution, where Y follows the exponential distribution with mean ξ_1 and Z is said to follow the exponential-GPD. The quantities $h(z)$ and $H(u)$ in Equation 7 are given by

$$\begin{aligned} h(z) &= 1/\xi_1 \times \exp(-z/\xi_1), \\ H(u) &= 1 - \exp(-u/\xi_1). \end{aligned} \quad (8)$$

The reason for such parameterisation will be seen in Section 3.

The majority of data for which the power law could be useful is usually discrete in nature, whether they are related to networks or not, as are the data sets in Figures 1 and 2. Therefore, it is not trivial to apply the extreme value mixture distribution in the literature that can be written as Equation 7, as they are for continuous data. To circumvent this issue, we will use the discretised version of the GPD proposed by Rohrbeck et al. (2018) for the tail. While the discrete power law no longer models the tail, it is retained in one of the proposed mixture distributions. Essentially, we are getting the best of both worlds, with the power law for the bulk of the data, and a distribution well established in extreme value theory for the tail. These discrete mixture distributions are introduced in the next section.

3 Discrete mixture distributions

In this section, we will derive two mixture distributions useful for discrete data such as those displayed in Section 1, namely the geometric-IGPD and the power-law-IGPD. A connection will be drawn to the exponential-GPD introduced in

Section 2. Finally, the likelihood based on these two mixture distributions will be derived.

A random variable X follows a discrete extreme value distribution if its probability mass function (PMF) is

$$p_X(x) = \begin{cases} (1 - \phi_u) \frac{H(x) - H(x-1)}{H(u)}, & x = 1, 2, \dots, u, \\ \phi_u [G_u(x) - G_u(x-1)], & x = u+1, u+2, \dots \end{cases} \quad (9)$$

where H is, as in Section 2, the CDF of a continuous distribution, and $G_u(z) = 1 - \left[1 + \frac{\xi_2(z-u)}{\sigma + \xi_2 u} \right]_+^{-1/\xi_2}$ is the CDF of the GPD, derived from integrating $g_u(z)$ in Equation 5 (under the current parameterisation). From the lower expression of Equation 9 we see that, conditional on $X > u$, X follows the integer-GPD (IGPD) introduced by Rohrbeck et al. (2018). The threshold u is assumed to be a positive integer, unlike in a continuous mixture distribution, where u can be a real number. Again the relevant limit is assumed if $\xi_2 = 0$. The survival function $S_X(x) = \Pr(X \geq x)$ can also be computed:

$$S_X(x) = \sum_{k=x}^{\infty} p_X(k) = \begin{cases} \phi_u + (1 - \phi_u) \left(1 - \frac{H(x-1)}{H(u)} \right), & x = 1, 2, \dots, u, \\ \phi_u \left[1 + \frac{\xi_2(x-1-u)}{\sigma + \xi_2 u} \right]_+^{-1/\xi_2}, & x = u+1, u+2, \dots \end{cases} \quad (10)$$

This will become useful when the form of $H(x)$ is given next.

3.1 Geometric distribution and IGPD

If H is the CDF of the geometric distribution with success probability p , we call that X follows the geometric-IGPD. The PMF $p_X(x)$ is such that

$$\begin{aligned} H(x) - H(x-1) &= p(1-p)^{x-1}, \\ H(u) &= 1 - (1-p)^u. \end{aligned} \quad (11)$$

If we reparametrise by $p = 1 - \exp(-1/\xi_1)$, with $\xi_1 > 0$ to ensure $p \in (0, 1)$, the upper expression of Equation 9 becomes

$$(1 - \phi_u) \frac{H(x) - H(x-1)}{H(u)} = (1 - \phi_u) \frac{[1 - \exp(-1/\xi_1)][\exp(-1/\xi_1)]^{x-1}}{1 - \exp(-u/\xi_1)}. \quad (12)$$

This completes the parameterisation of the geometric-IGPD, which is not only for alignment with the other distribution to be introduced, but also for connecting with the exponential-GPD introduced in Section 2. Specifically, if a continuous random variable Z follows the exponential-GPD given by Equations 7 and 8, and X follows the geometric-IGPD given by Equations 9 and 11, then integrating $f_Z(z)$ over the unit interval $[x-1, x]$ yields $p_X(x)$:

$$p_X(x) = \int_{x-1}^x f_Z(z) dz, \quad (13)$$

which means the two random variables X and $\lceil Z \rceil$ are identically distributed. In other words, if Z follows the exponential-GPD with parameters $(\xi_1, \xi_2, \sigma, u, \phi_u)$, then $\lceil Z \rceil$ follows the geometric-IGPD with the same set of parameters. Essentially, the latter distribution can be seen as a discretisation of the former. The parametrisation that uses ξ_1 instead of p not only gives ξ_1 a meaning, which is the expectation of the bulk exponential distribution, but also aligns with the parametrisation of distribution to be introduced next, which is a mixture of the discrete power law and the IGPD. One final note is that the exponential-GPD is a special case of the Gamma-GPD, which has been used by Behrens et al. (2004).

3.2 Discrete power law and IGPD

Consider a discrete random variable X that follows the power law if $X \leq u$ and the IGPD if $X > u$. This means $p_X(x)$ in Equation 9 is such that

$$\begin{aligned} H(x) - H(x-1) &= x^{-1/\xi_1-1}, \\ H(u) &= \zeta(1/\xi_1 + 1, 1) - \zeta(1/\xi_1 + 1, u+1), \end{aligned} \tag{14}$$

where $\xi_1 > 0$ (unlike ξ_2 which is unbounded). We say that X follows the (discrete) power-law-IGPD. The term ‘‘discrete’’ is dropped hereafter. That the power law for the bulk distribution is parametrised in this way is because, in its continuous version, having an exponent of $1/\xi_1 + 1$ is equivalent to following the GPD with shape ξ_1 , by comparing Equations 1 and 6. As the tail is modelled by the (I)GPD with shape parameter ξ_2 , that $\xi_1 = \xi_2$ is a necessary condition that the power law is adequate for the whole of the data. This will be examined in the application in Section 5. Unlike the geometric-IGPD, this power-law-IGPD cannot be derived from discretising the mixture of the continuous power law distribution and the GPD. The reason for this is that the integral $\int_0^\infty x^{-1/\xi_1-1} dx$ which is required to discretise the power-law distribution is not finite, and hence the continuous power law with $u = 0$ cannot be normalised to be a proper density function. Additionally, unlike their continuous counterparts, the IGPD does not generalise the discrete power law. Rather, the IGPD discretises the GPD, which in turn generalises the continuous power law.

The two extreme value mixture distributions, namely geometric-IGPD and power-law-IGPD, have the same set of parameters $(\xi_1, \xi_2, \sigma, u, \phi_u)$. Furthermore, they have the same parameter space for ξ_1 , which is the positive real line. While their values of ξ_1 are not directly comparable, such alignment in the parametrisation allows for a unified inference framework in Section 4. The two distributions also have the same support on positive integers. Note that 0 is excluded because the PMF at 0 would be problematic for the power-law-IGPD. In the presence of 0’s in the data, the probability of observing 0 can be estimated separately, while the appropriate mixture distribution is fitted to the rest of the data.

3.3 Likelihood and continuity constraint

If we have a sample of size n , denoted by $\mathbf{x} = (x_1, x_2, \dots, x_n)$, assumed to come from the discrete mixture distribution given by Equation 9, we can derive the likelihood:

$$\begin{aligned}
L(\xi_1, \xi_2, \sigma, u | \mathbf{x}) &= \prod_{i=1}^n p_X(x_i) \\
&= \prod_{i:x_i \leq u} (1 - \phi_u) \frac{H(x_i) - H(x_i - 1)}{H(u)} \times \prod_{i:x_i > u} \phi_u [G_u(x_i) - G_u(x_i - 1)] \\
&= (1 - \phi_u)^{n - n_u} \phi_u^{n_u} \times \prod_{i:x_i \leq u} \frac{H(x_i) - H(x_i - 1)}{H(u)} \prod_{i:x_i > u} [G_u(x_i) - G_u(x_i - 1)],
\end{aligned} \tag{15}$$

where $n_u = \mathbf{1}_{\{x_i \leq u\}}$, and $\mathbf{1}_{\{A\}}$ is the indicator function of event A . The parameters ξ_1 and (ξ_2, σ) describe the bulk distribution (geometric or power law) and the IGPD, respectively, while u will also be treated as a parameter, as quantifying the threshold uncertainty is one main goal of using these mixture distributions. The likelihood factorises into a function of ϕ_u and a function of the remaining parameters, and so ϕ_u can be estimated separately with its MLE n_u/n i.e. the empirical proportion of exceedances. One drawback with this treatment of ϕ_u is that it is data-dependent. Without the MLE of ϕ_u according to the data, quantities such as the PDF $p_X(x)$ in Equation 9 cannot be evaluated. A common alternative is to impose a continuity constraint of the *density* function at u , so that ϕ_u is not a free parameter but derived from u (and other parameters). For a comparison of the mixture distribution with and without constraints, please see Scarrott and MacDonald (2012).

For the geometric-IGPD, we impose the continuity constraint to its continuous counterpart (exponential-GPD), which, according to Equation 7, leads to

$$(1 - \phi_u) \times \frac{1/\xi_1 \times \exp(-u/\xi_1)}{1 - \exp(-u/\xi_1)} = \phi_u \times \frac{1}{\sigma_u},$$

and therefore

$$\phi_u = \left\{ 1 + \frac{\xi_1}{\sigma_u} \left[\exp \left(\frac{u}{\xi_1} \right) - 1 \right] \right\}^{-1}. \tag{16}$$

The power-law-IGPD is not derived from discretising a respective continuous mixture distribution, so we introduce a constraint that $p_X(u+1)$, given by the lower expression in Equation 9, is equal to what the upper expression would have been, *had the power law been extended beyond u* . Using Equations 9 and 14, we have

$$\frac{(1 - \phi_u) \times (u+1)^{-1/\xi_1 - 1}}{\zeta(1/\xi_1 + 1, 1) - \zeta(1/\xi_1 + 1, u+1)} = \phi_u \times \left\{ 1 - \left[1 + \frac{\xi_2}{\sigma + \xi_2 u} \right]_+^{-1/\xi_2} \right\},$$

and therefore

$$\phi_u = \left\{ 1 + \frac{(u+1)^{1/\xi_1+1} \left\{ 1 - \left[1 + \frac{\xi_2}{\sigma + \xi_2 u} \right]_+^{-1/\xi_2} \right\}^{-1}}{[\zeta(1/\xi_1+1, 1) - \zeta(1/\xi_1+1, u+1)]^{-1}} \right\}^{-1}. \quad (17)$$

For both mixture distributions, both the unconstrained version, where ϕ_u is a free parameter, and the constrained version, using Equations 16 and 17 respectively, will be applied in Section 5.

4 Inference

In this section we will outline the inference algorithm, which can be applied directly and separately to both the geometric-IGPD and the power-law-IGPD introduced in Section 3. For each distribution, the constrained and unconstrained versions will be unified in the inference framework. However, the two *distributions* will not be unified in the inference algorithm for the purpose of model selection *between* the distributions.

Provided that the threshold u is known and since (ξ_1, σ) are involved only in the bulk and tail distributions, respectively, their MLE can be obtained by maximising $\prod_{i:x_i \leq u} \frac{H(x_i) - H(x_i-1)}{H(u)}$ and $\prod_{i:x_i > u} [G_u(x_i) - G_u(x_i-1)]$ in Equation 15 separately. Substituting this back to Equation 15 enables us to obtain the profile likelihood of u , and hence the MLE of u . As ϕ_u is involved in the likelihood and thus the profile likelihood, the MLE of u may be different between the constrained and unconstrained versions for ϕ_u .

While this approach is computationally highly efficient, the uncertainty around u cannot be quantified by using the asymptotic Gaussianity of the MLE, as the regularity conditions required do not hold. For example, the profile (log-)likelihood over u usually has discontinuities at several thresholds and is therefore not differentiable. Therefore, to quantify the threshold uncertainty, we consider the Bayesian approach, to obtain the full joint posterior of $(\xi_1, \xi_2, \sigma, u)$ and hence quantify the threshold uncertainty can then be quantified according to the marginal posterior of u .

Priors have to be assigned to the free parameters before carrying out Bayesian inference. Denote the continuous uniform distribution with lower bound a and b by $U(a, b)$, the Gaussian distribution with expectation m and variance s^2 by $N(m, s^2)$, and the Gamma distribution with shape parameter a and scale parameter b by $\text{Gamma}(a, b)$. Independent and relatively uninformative priors are specified as follows:

$$\begin{aligned} \xi_1 &\sim U(a_{\xi_1} = 0, b_{\xi_1} = 100), \\ \xi_2 &\sim N(m_{\xi_2} = 0, s_{\xi_2}^2 = 30^2), \\ \sigma &\sim \text{Gamma}(a_\sigma = 1, b_\sigma = 0.01), \\ \phi_u &\sim U(a_\phi = 0.005, b_\phi = 0.4). \end{aligned} \quad (18)$$

Note that the prior for u is specified indirectly through that for ϕ_u , because the support for u depends on the scale of the data, whereas $\phi_u \in [0, 1]$ regardless of this. As ϕ_u depends on u in both the constrained and unconstrained versions, the number of free parameters stays the same as the number of priors. We refer to the constrained and unconstrained versions by $M = 1$ and $M = 0$, respectively, where M represents the choice of the *model*, and subscript the corresponding likelihood and posterior density by the value of M .

Using Bayes' theorem, the joint posterior of the parameters is the product of the likelihood and the joint prior of the parameters, up to a proportionality constant. Specifically, for $M = 0, 1$,

$$\pi_M(\xi_1, \xi_2, \sigma, u | \mathbf{x}) \propto L_M(\xi_1, \xi_2, \sigma, u | \mathbf{x}) \times \pi(\xi_1)\pi(\xi_2)\pi(\sigma)\pi(\phi_u), \quad (19)$$

which can be computed using Equations 15 and 18. As the proportionality constant is usually computationally intractable, one natural way of drawing samples from this joint posterior is Markov chain Monte Carlo (MCMC). For detailed recipes and practical considerations of MCMC, please see, for example, Gamerman and Lopes (2006). Within the MCMC framework, a Metropolis-within-Gibbs algorithm is implemented here for the mixture distributions, and is detailed in the Appendix A.

Solely for the purpose of inference and model selection, the constrained and unconstrained versions are unified in the algorithm. This is achieved by introducing the priors for the model $\pi(M = 1)$ and $\pi(M = 0)$. Upon obtaining the MCMC output, the empirical proportions of 1's and 0's are the estimates of the posterior probabilities of the versions with and without the continuity constraint, denoted by $\hat{\pi}(M = 1 | \mathbf{x})$ and $\hat{\pi}(M = 0 | \mathbf{x})$, respectively. Together with their prior probabilities, we can calculate the Bayes factor

$$B_{01} = \frac{\hat{\pi}(M = 0 | \mathbf{x})}{\hat{\pi}(M = 1 | \mathbf{x})} \Big/ \frac{\pi(M = 0)}{\pi(M = 1)},$$

which can be used for model selection between $M = 1$ and $M = 0$. It should be noted that, given the same parameter values, the likelihood under no constraint is always greater than or equal to the constrained counterpart. As the Bayes factor is the ratio of the marginal likelihoods, by construction B_{01} is always greater than or equal to 1. Therefore, we should use the Bayes factor to determine how much better it is without the constraint than with the constraint, instead of always selecting the former. Nevertheless, this decision must account for both the Bayes factor and the fact that the constrained version is not data-dependent.

If we split the MCMC output according to M , we obtain one set of samples from the joint posterior $\pi_1(\xi_1, \xi_2, \sigma, u | \mathbf{x})$ and another from $\pi_0(\xi_1, \xi_2, \sigma, u | \mathbf{x})$. Using the former for example, we can obtain, for each $x = 1, 2, \dots$, the posterior distribution of $p_X(x)$ in Equation 9 and $S_X(x)$ in Equation 10, under the version with continuity constraint. These two quantities will be of interest as the goodness of fit of the distribution can be examined visually by, for example, comparing the credible intervals of $S_X(x)$ with the empirical survival functions. Such examination will be carried out in Section 5, alongside that of the posterior distribution of the parameters.

5 Application

In this section, the results obtained from fitting the two extreme value mixture distributions to the data presented in Section 1 are shown, focusing on the goodness-of-fit of the proposed distributions, and on the posterior of the shape parameters ξ_1 and ξ_2 and the threshold u . Supplementary plots are provided in Appendix B.

The three sets of data in the first row of Figures 1 and 2 are modelled by the geometric-IGPD, as their left tails seem not to obey the power law, while those in the second row are modelled by the power-law-IGPD, as their left tails do seem to obey the power law. For each data set, the MCMC algorithm for the corresponding distribution is run for 2020000 iterations, with the first 20000 discarded as burn-in, and the rest thinned by 100 to achieve good mixing and obtain a chain of length 20000.

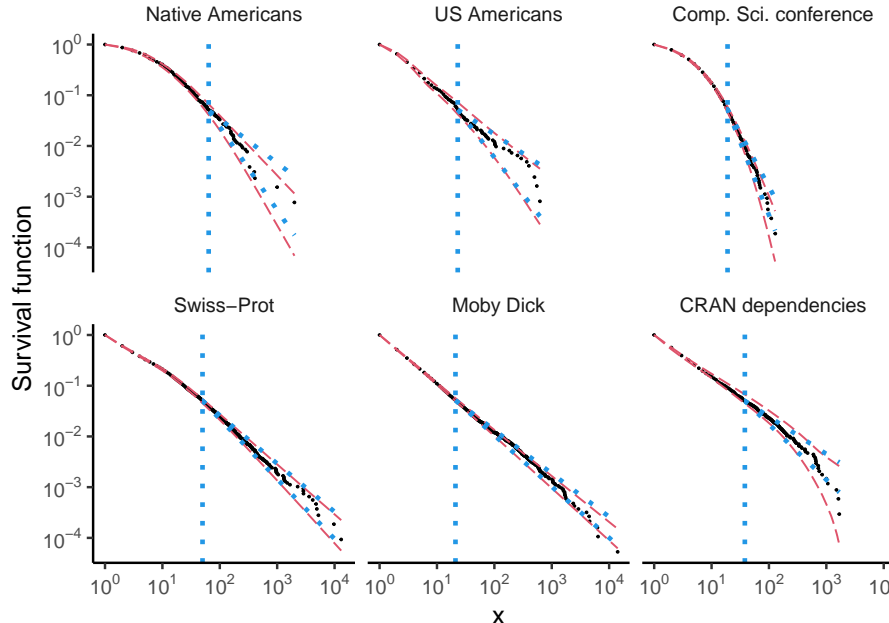


Figure 3: Survival function with credible intervals according to the mixture distributions with continuity constraint (red, dashed) and the discrete power law (blue, dotted) with 95% threshold (vertical).

For each integer value within the data range, the posterior distribution of the fitted survival function $S_X(x)$ is calculated, of which the 99% credible intervals are shown in Figure 3, for the version with continuity constraint. The fit by the unconstrained version is highly similar and is therefore not shown. That almost all the data points lie within the credible intervals, as well as their narrow width, suggests a good fit of the mixture distributions. Note that only the survival function is shown here because it is a better quantity for assessing the goodness of fit when the right tail is of greater interest than the bulk. The corresponding

plot of the credible intervals of the fitted frequencies encompassing the empirical frequencies is shown in Figure 13 in Appendix B. Also overlaid are the credible intervals obtained by fitting the discrete power law to the observations above the fixed 95% quantile. The mixture distributions are as good as the discrete power law in all cases, and provide a clearly better fit for CRAN dependencies, all without a subjective choice of u or throwing away subsets of data.

5.1 Adequacy of the power law alone

One question to be answered, in the cases where the power-law-IGPD is fitted, is whether the power law alone is sufficient to describe the whole of the data. This would be indicated by the proximity of the shape parameters of the two components in the mixture distribution. The posterior densities of ξ_1 and ξ_2 , plotted in Figure 4 for conciseness, suggest otherwise. It can be clearly seen that ξ_1 stochastically dominates ξ_2 *aposteriori*, for both versions with and without the continuity constraint. Such stochastic dominance is particularly important for Swiss-Prot and Moby Dick data, where the power-law-IGPD is fitted. Using the power law implied by ξ_1 for the whole of the data would mean a heavier tail than that by the IGPD, which, according to Figure 3, fits the data very well. While the power law is powerful in describing the bulk of the data using one parameter only, the more flexible IGPD is more appropriate when it comes to the right tail.

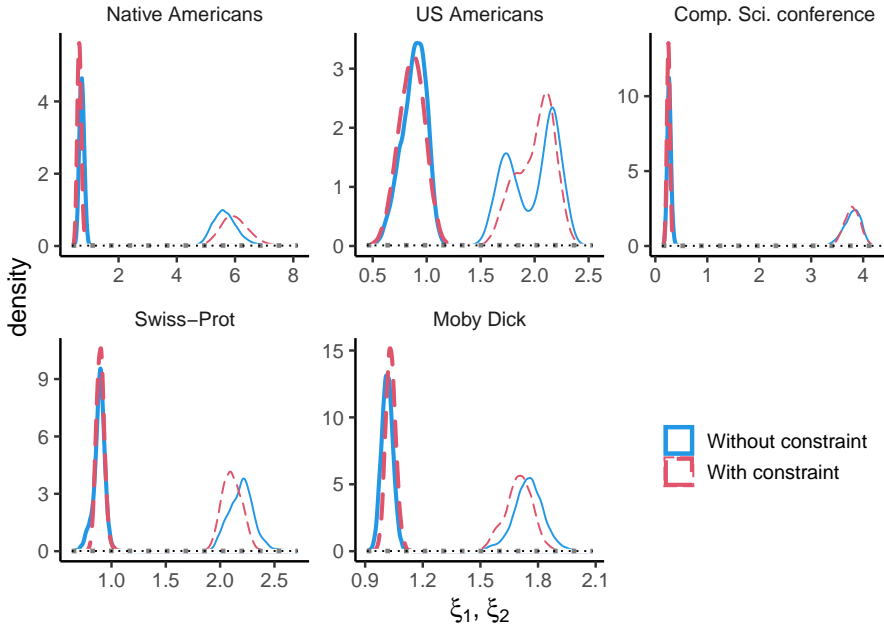


Figure 4: Prior (grey, dotted) and posterior of ξ_1 (thin) and ξ_2 (bold), with (red, dashed) and without (blue, solid) continuity constraint.

Another indication of whether the power law alone is adequate is the poste-

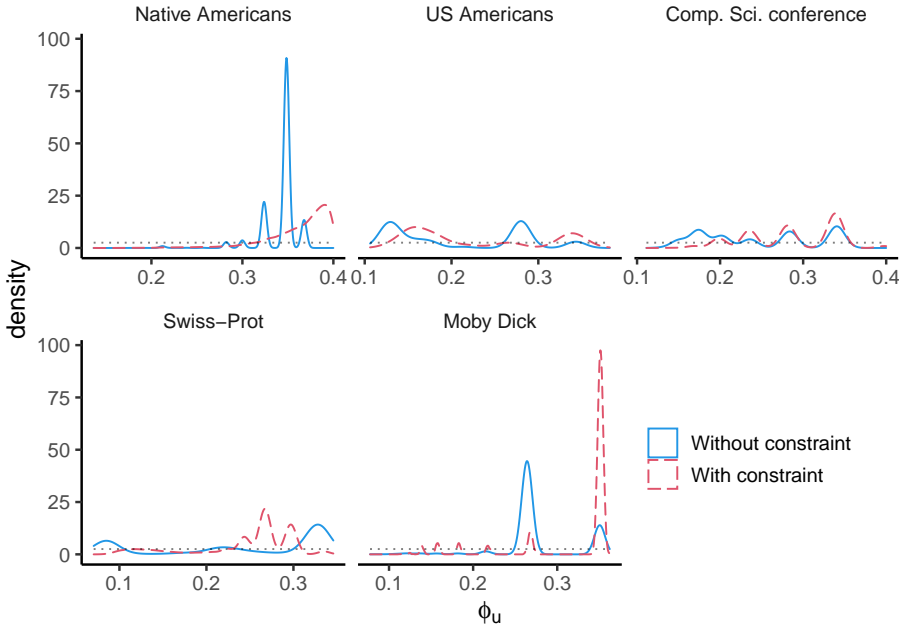


Figure 5: Prior (grey, dotted) and posterior of ϕ_u , with (red, dashed) and without (blue, solid) continuity constraint.

prior distribution of ϕ_u , again in the cases where the power-law-IGPD is fitted. A posterior density concentration towards $a_\phi = 0.005$, the lower end point of the prior, would mean that the power law pushes the IGPD towards the extremes of the data. From the second row of Figure 5, this is not the case, reinforcing the argument that the IGPD is required for the right tail. By observing the first row of the same figure, this argument is also valid for the cases where the geometric-IGPD is fitted. Another observation from Figure 5 is the discreteness and multi-modality of the posterior of ϕ_u under the version without continuity. This arises because the estimate is the empirical proportion of threshold exceedances. The numbers of unique values of ϕ_u in the six data sets are 16, 9, 8, 31, 12, 135, respectively in the order they are presented.

5.2 Adequacy of IGPD alone and threshold uncertainty

As the posterior of ϕ_u pushes towards the upper bound $b_\phi = 0.4$ in most cases, it seems like the IGPD is indeed sufficient for not only the tail but also a larger proportion of the data. This leads well to the examination of threshold uncertainty through the posterior of PMF of u , which is plotted in Figure 6. These figures depict a similar picture to Figure 5, but on the original scale of the data. In most cases the posterior of u is concentrated on values below 10, which however is perfectly reasonable due to how the observed data is distributed. The proportion of data smaller than or equal to 2 in the six data sets, after excluding the 0's, are 0.235, 0.55, 0.381, 0.544, 0.649, 0.606, respectively in the

order they are presented.

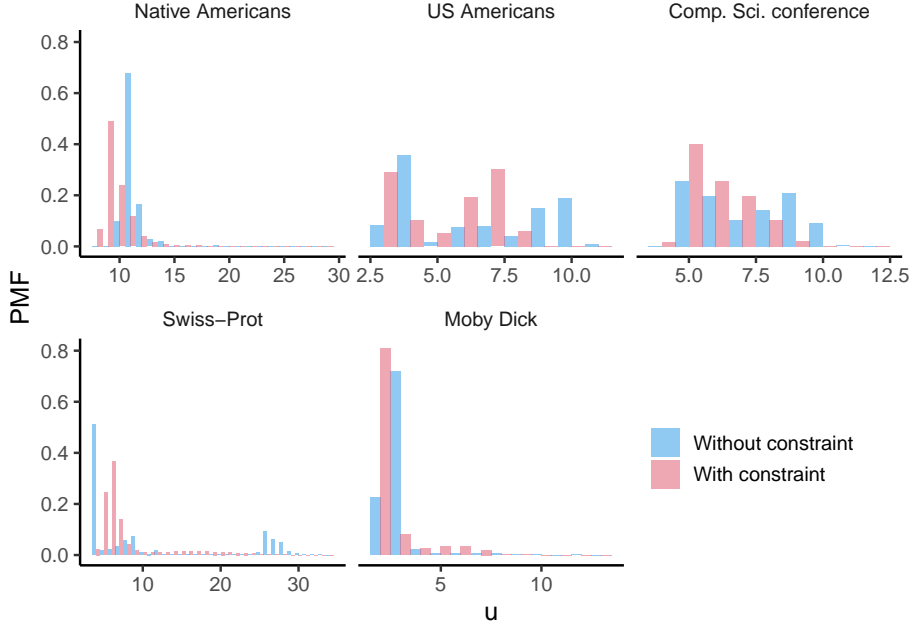


Figure 6: Posterior PMF of u .

The wide range of values for the posterior of u and the existence of multiple modes in some cases illustrates the threshold uncertainty well, and the need of the mixture distributions. However, in some cases, such as Moby Dick with continuity constraint, and the computer science conference and Swiss-Prot without continuity constraint, the lowest threshold possible is the posterior mode. This is echoed by looking at the log-posterior density *conditional on each u* in the ridge plots in Figures 7 and 8. That the posterior density attains maximum at the lowest threshold possible indicates a possibility of using the IGPD for the whole of the data. Nevertheless, the threshold uncertainty is more prominent when it comes to the posterior density on the log scale, and therefore should be examined in this way when fitting the mixture distributions.

5.3 CRAN dependencies

The corresponding plots for CRAN dependencies are omitted in Figures 4, 5, 6, 7 and 8 because visible examination is difficult on the same scale as the other data sets. Therefore, we plot the posterior of ξ_1 on the log scale on the left of Figure 9, and the posterior of ϕ_u on the right, corresponding to Figures 4 and 5, respectively. The posterior of ξ_2 is not shown because there are negative values sampled, but the stochastic dominance of ξ_1 over ξ_2 still holds. For the version without the continuity constrain, the posterior of ξ_1 shows a long right tail, due to comparable levels of the (log-)posterior density at large values of ξ_1 at the lowest possible threshold $u = 2$. For comparison, the maximum values in the

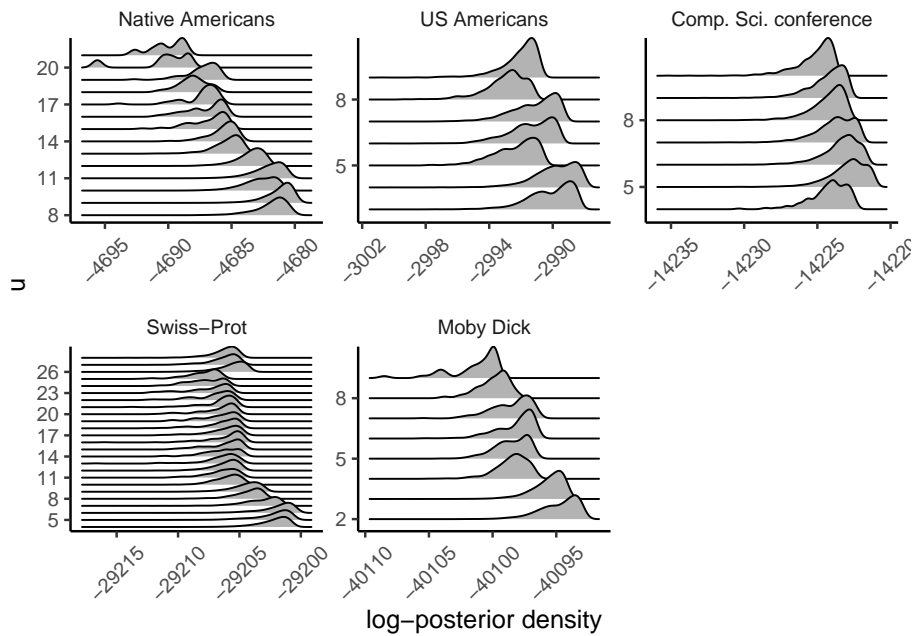


Figure 7: Ridge plot for log-posterior at different u with continuity constraint.

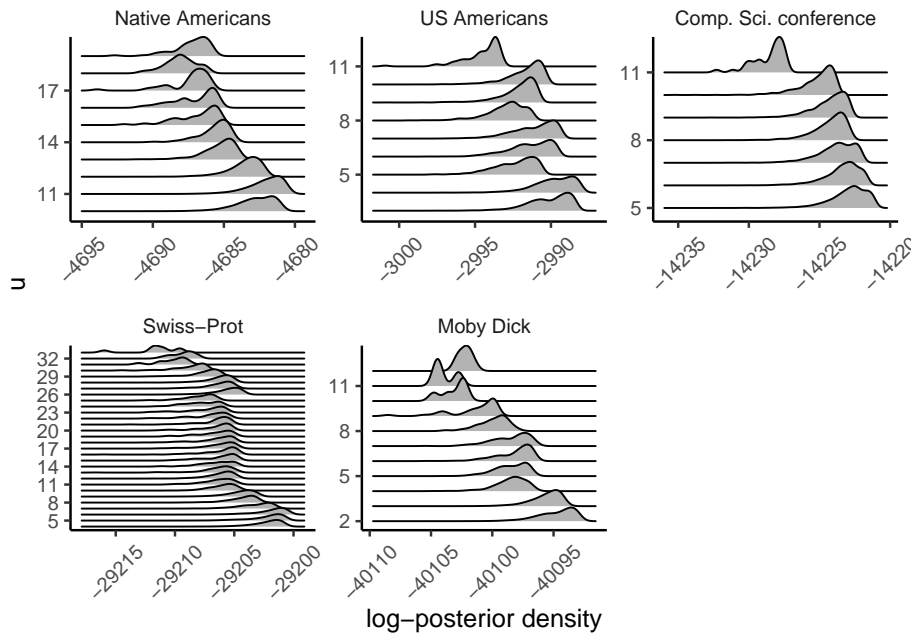


Figure 8: Ridge plot for log-posterior at different u without continuity constraint.

MCMC output with and without the continuity constraint are 2.499 and 8.215, respectively.

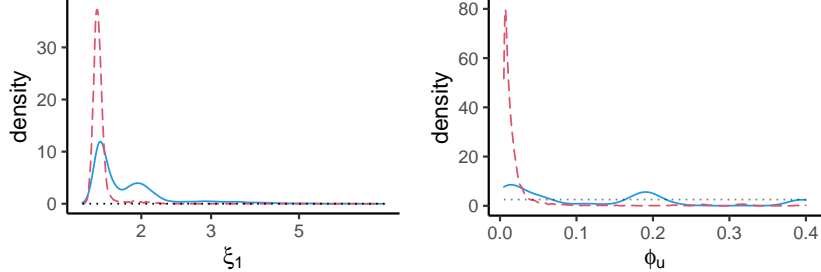


Figure 9: Prior (grey, dotted) and posterior of ξ_1 (left) and ϕ_u (right), with (red, dashed) and without (blue, solid) continuity constraint, for CRAN dependencies.

We plot the posterior of u *on the log scale* for CRAN dependencies in Figure 10. This shows larger threshold uncertainty than seen in Figure 6. The posterior modes for the versions with and without continuity constraint are 3 and 6, respectively, which are close but not equal to the lowest threshold possible. Such phenomenon and the existence of a secondary mode within a wider range of large values echo the general phenomenon seen in other data sets, with or without the continuity constraint. The use of the mixture distributions enables multiple modes to be discovered and compared.

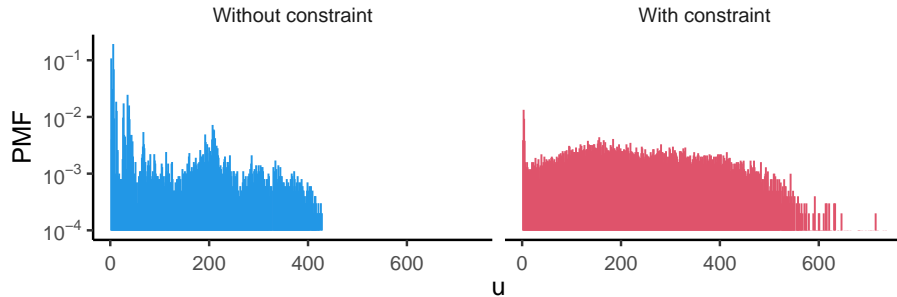


Figure 10: Posterior PMF of u for CRAN dependencies.

5.4 Comparison with existing results for Moby Dick data

It is useful to compare our results with those by, for example, Gillespie (2015), who fitted the power law to the Moby Dick data above a threshold, and quantified the threshold uncertainty by a bootstrap procedure. According to their Figure 2, the mean and the standard deviation of the threshold are 6.5 and 1.8, respectively. From the bottom-middle histograms in Figure 6, the power-law-IGPD opted for a lower threshold. It is worth noting the difference that the

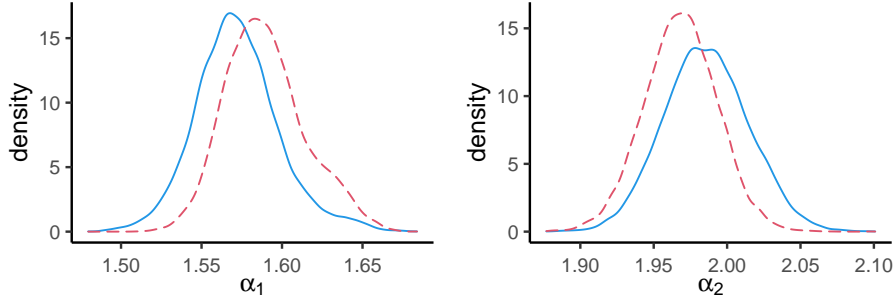


Figure 11: Posterior for the exponents implied by ξ_1 (left) and ξ_2 (right), with (red, dashed) and without (blue, solid) continuity constraint, for the Moby Dick data.

power law is fitted to the observations below u in our application and above u in theirs.

For comparison we plot the posterior density of the exponents *implied by the shape parameters*, that is, $\alpha_1 = 1/\xi_1 + 1$ and $\alpha_2 = 1/\xi_2 + 1$, in Figure 11. The posterior of α_2 agrees broadly with the results reported by Gillespie (2015), with a mean of 1.947 and a standard deviation of 0.024, which indicates that both the IGPD in the mixture distribution and the power law alone captured the same right tail behaviour. Nevertheless, the mixture distribution is more flexible, and simultaneously allows for a different power law in the bulk of the data. Lastly, we plot α_2 against u in Figure 12. This is comparable to Figure 3(c) in Gillespie (2015), and shows that the exponent, or equivalently the shape parameter, is relatively stable at different values of u .

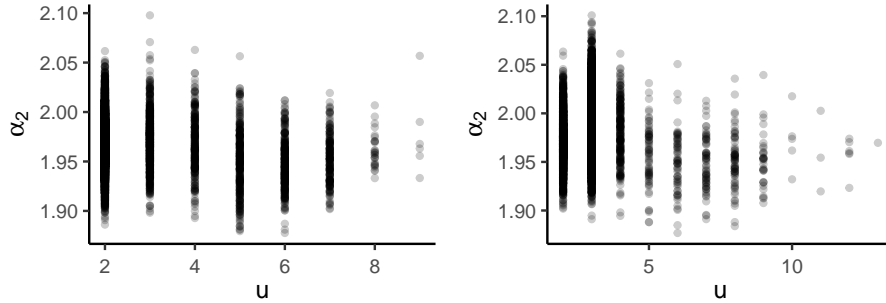


Figure 12: Scatterplot of $\alpha_2 = 1/\xi_2 + 1$ against u , with (left) and without (right) continuity constraint, for the Moby Dick data.

Whilst not directly comparable, we also report the Kolmogorov-Smirnov statistic for the fit of each data set in Table 1. This statistic is essentially the maximum absolute difference between the empirical and fitted survival functions, and is denoted by KS_1 and KS_0 for the versions with or without the continuity constraint, respectively. The fitted survival function is calculated using the mode of the joint posterior of the parameters. For all data sets considered,

Data	KS_1	KS_0	B_{01}
Native Americans	0.02 (10)	0.018 (5)	21.54
US Americans	0.015 (7)	0.014 (12)	10.73
Comp. Sci. conference	0.008 (3)	0.007 (3)	3.84
Swiss-Prot	0.006 (3)	0.006 (3)	38.66
Moby Dick	0.002 (7)	0.002 (16)	10.97
CRAN dependencies	0.008 (2)	0.008 (3)	11.06

Table 1: The Kolmogorov-Smirnov statistics for the version with (KS_1) and without (KS_0) the continuity constraint, and the Bayes factor (B_{01}) for the latter relative to the former.

this statistic in the version without continuity constraint (KS_0) is smaller than or equal to the constrained counterpart (KS_1), although this does not necessarily hold for any data. The integer in the parentheses is the value where such absolute difference is maximised.

5.5 Model selection for continuity constraint

Also reported in Table 1 is the Bayes factor (B_{01}), for comparing the versions with and without the continuity constraint. Echoing the argument in Section 4, B_{01} is greater than 1 for all data sets. Using the categorisation by Kass and Raftery (1995), while there is positive evidence for the unconstrained version, such evidence is considered strong enough only for the Swiss-Prot data and possibly the Native Americans data. As using the constrained version does not lead to substantial difference in terms of the fitted values, a slight preference is given to the constrained version, if it does not provide a (visually) much worse fit, because it is not data-dependent and therefore can be used for simulation, for example. Additionally, as discussed in relation to Figure 5, under the version without the continuity constraint, ϕ_u can only take values $\left\{ \frac{\lceil a_\phi n \rceil}{n}, \frac{\lceil a_\phi n \rceil + 1}{n}, \dots, \frac{\lfloor b_\phi n \rfloor - 1}{n}, \frac{\lfloor b_\phi n \rfloor}{n} \right\}$ due to its definition as the empirical proportion of exceedances, and is therefore technically discrete. This is not an issue for the version with the continuity constraint, which can take any real value between a_ϕ and b_ϕ .

6 Discussion

The results in Section 5 support the use of the mixture distributions. They provide a very good fit to both the bulk and the tail of the data, while quantifying the uncertainty of threshold, without throwing away some data points according to a subjective decision. Neither the power law nor the geometric distribution alone is adequate to describe the whole of the data. Also, neither is the power law sufficient to describe the (right) *tail* of the data, which is usually lighter than what would have been expected from the decay of the bulk of the data. This tail is better captured by the IGPD, which is approximately a generalisation of the discrete power law, as the continuous version of the former

(the GPD) is indeed a generalisation of the continuous version of the latter (the Pareto distribution).

The IGPD alone seems sufficient without being as part of a mixture distribution. The main drawback is that any threshold uncertainty will not be quantified. This also amounts to assuming that the whole of the data indeed follows the IGPD, and that the asymptotics concerning the exceedances of a *high* threshold still holds with a very low or even no threshold. Such assumptions will need to be supported by the theory, before using the IGPD alone instead of incorporating it in a mixture distribution.

While the continuous counterparts of the mixture distributions, that is, the exponential-GPD and the continuous-power-law-GPD, could be further developed, we argue that the discrete cases presented are more widely applicable. In the contexts where the power law is of interest, the data are usually discrete in nature. Furthermore, in the case of the continuous-power-law-GPD, the integral of the continuous power law on the positive real line is not finite. This outstanding issue needs to be resolved before the continuous mixture distribution can be applied without an arbitrary and subjective lower cut-off point.

As the mixture distributions manage to describe network in-degrees well, one natural question is, what generative model does a given combination of the parameters correspond to? For example, can the preferential attachment model, of which the original version implies a power law with exponent $2 < \alpha < 3$ or equivalently $1 > \xi_1 > 0.5$, be modified so that the resulting network has the desired degree distribution? Nevertheless, the rules of new nodes joining a network and connecting with existing nodes are beyond the scope of the current paper.

In Section 4 we have seen that the two versions with and without continuity constraint are unified in the inference algorithm, by treating the constraint as an extra parameter, thus allowing the MCMC output to be used for model selection. It would also be possible unify the geometric-IGPD and the power-law-IGPD in the MCMC algorithm, by incorporating another step for the extra binary parameter that represents the *distribution*. The MCMC output can then be used for model selection between the two *distributions*. As the parameter space and prior, in particular those of ξ_1 , are aligned, transdimensional MCMC will not be needed. However, as there are clear indications on the appropriate choice of the mixture distribution according the frequency plots in Figure 1, such model selection procedure within the inference algorithm will not be necessary in our application.

References

Albert, R., Jeong, H. and Barabási, A.-L. (1999), ‘Internet: Diameter of the world-wide web’, *Nature* **401**, 130–131.

Albert, R., Jeong, H. and Barabási, A.-L. (2000), ‘Error and attack tolerance of complex networks’, *Nature* **406**, 378–382.

Alstott, J., Bullmore, E. and Plenz, D. (2014), ‘powerlaw: A python package for analysis of heavy-tailed distributions’, *PLoS ONE* **9**(1), e85777.

Arroyo-Machado, W., Torres-Salinas, D., Herrera-Viedma, E. and Romero-Frías, E. (2020), ‘Science through Wikipedia: A novel representation of open knowledge through co-citation networks’, *PLOS One* **15**(2), e0228713.

Barabási, A.-L. and Albert, R. (1999), ‘Emergence of scaling in random networks’, *Science* **286**(5439), 509–512.

Bavota, G., Canfora, G., Di Penta, M., Oliveto, R. and Panichella, S. (2015), ‘How the apache community upgrades dependencies: an evolutionary study’, *Empirical Software Engineering* **20**, 1275–1317.

Baxter, G., Frean, M., Noble, J., Rickerby, M., Smith, H., Visser, M., Melton, H. and Tempero, E. (2006), Understanding the shape of Java software, in ‘OOPSLA ’06: Proceedings of the 21st annual ACM SIGPLAN conference on Object-oriented programming systems, languages, and applications’, pp. 397–412.

Behrens, C. N., Lopes, H. F. and Gamerman, D. (2004), ‘Bayesian analysis of extreme events with threshold estimation’, *Statistical Modelling* **4**, 227–244.

Bell, M. J., Gillespie, C. S., Swan, D. and Lord, P. (2012), ‘An approach to describing and analysing bulk biological annotation quality: A case study using UniProtKB’, *Bioinformatics* **28**(18), i562–i568.

Bessi, A. (2015), ‘Two samples test for discrete power-law distributions’, *ArXiv e-prints* . arXiv:1503.00643.

Bhamidi, S., Steele, J. M. and Zaman, T. (2015), ‘Twitter event networks and the Superstar model’, *The Annals of Applied Probability* **25**(5), 2462–2502.

Bohorquez, J. C., Gourley, S., Dixon, A. R., Spagat, M. and Johnson, N. F. (2009), ‘Common ecology quantifies human insurgency’, *Nature* **462**(7275), 911–914.

Bollobás, B., Borgs, C., Chayes, J. and Riordan, O. (2003), Directed scale-free graphs, in ‘Proceedings of the Fourteenth Annual ACM-SIAM Symposium on Discrete Algorithms’, ACM, New York, pp. 132–139.

Broido, A. D. and Clauset, A. (2019), ‘Scale-free networks are rare’, *Nature Communications* **10**(1017).

Carreau, J. and Bengio, Y. (2009), ‘A hybrid Pareto model for asymmetric fat-tailed data: the univariate case’, *Extremes* **12**, 53–76.

Clauset, A., Shalizi, C. R. and Newman, M. E. J. (2009), ‘Power-law distributions in empirical data’, *SIAM Review* **51**(4), 661–703.

Coles, S. (2001), *An Introduction to Statistical Modeling of Extreme Values*, Springer Series in Statistics, Springer.

Corral, A., Deluca, A. and Ferrer-i-Cancho, R. (2012), ‘A practical recipe to fit discrete power-law distributions’, *ArXiv e-prints* . arXiv:1209.1270.

Cox, J., Bouwers, E., van Eekelen, M. and Visser, J. (2015), Measuring dependency freshness in software systems, in ‘2015 IEEE/ACM 37th IEEE International Conference on Software Engineering’, Vol. 2, pp. 109–118.

de Solla Price, D. (1976), ‘A general theory of bibliometric and other cumulative advantage processes’, *Journal of the Association for Information Science and Technology* **27**(5), 292–306.

do Nascimento, F. F., Gamerman, D. and Lopes, H. F. (2012), ‘A semiparametric Bayesian approach to extreme value estimation’, *Statistics and Computing* **22**, 661–675.

Faloutsos, M., Faloutsos, P. and Faloutsos, C. (1999), On power-law relationships of the internet topology, in ‘Proceedings of the Conference on Applications, Technologies, Architectures, and Protocols for Computer Communication’, SIGCOMM ’99, ACM, New York, NY, USA, pp. 251–262.

Friedman, J. A. (2015), ‘Using power laws to estimate conflict size’, *Journal of Conflict Resolution* **59**, 1216–1241.

Frigessi, A., Haug, O. and Rue, H. (2002), ‘A dynamic mixture model for unsupervised tail estimation without threshold selection’, *Extremes* **5**, 219–235.

Gamerman, D. and Lopes, H. F. (2006), *Markov Chain Monte Carlo: Stochastic Simulation for Bayesian Inference*, 2nd edn, Chapman & Hall/CRC.

Gillespie, C. S. (2015), ‘Fitting heavy tailed distributions: the poweRlaw package’, *Journal of Statistical Software* **64**(2), 1–16.
URL: <http://www.jstatsoft.org/v64/i02/>

Gillespie, C. S. (2017), ‘Estimating the number of casualties in the American Indian war: a Bayesian analysis using the power law distribution’, *Annals of Applied Statistics* **11**(4), 2357–2374.

Hill, B. M. (1975), ‘A simple general approach to inference about the tail of a distribution’, *The Annals of Statistics* **3**(5), 1163–1174.

Hsiao, P.-N., Tsai, Y., Huang, W.-F. and Lin, C.-C. (2007), A growing network model with high hub connectivity and tunable clustering coefficient, in ‘The 9th International Conference on Advanced Communication Technology’, Vol. 3, pp. 2171–2175.

Hu, Y. and Scarrott, C. (2018), ‘evmix: An R package for extreme value mixture modeling, threshold estimation and boundary corrected kernel density estimation’, *Journal of Statistical Software* **84**(5), 1–27.

Jenkins, S. and Kirk, S. R. (2007), ‘Software architecture graphs as complex networks: A novel partitioning scheme to measure stability and evolution’, *Information Sciences* **177**, 2587–2601.

Ji, P. and Jin, J. (2016), ‘Coauthorship and citation networks for statisticians’, *Annals of Applied Statistics* **10**(4), 1779–1812.

Jóhannesson, G., Björnsson, G. and Gudmundsson, E. H. (2006), ‘Afterglow light curves and broken power laws: a statistical study’, *The Astrophysical Journal Letters* **640**(1).

Kass, R. E. and Raftery, A. E. (1995), ‘Bayes factors’, *Journal of the American Statistical Association* **90**(430), 773–795.

Kohring, G. A. (2009), ‘Complex dependencies in large software systems’, *Advances in Complex Systems* **12**(06), 565–581.

Krapivsky, P. L. and Redner, S. (2001), ‘Organization of growing random networks’, *Physical Review E* **63**(6), 066123.

Krapivsky, P. L., Rodgers, G. J. and Redner, S. (2001), ‘Degree distributions of growing networks’, *Physical Review Letters* **86**(23), 5401–5404.

LaBelle, N. and Wallingford, E. (2004), ‘Inter-package dependency networks in open-source software’, *ArXiv e-prints* . arXiv:cs/0411096.

Lee, C. (2020), *crandep: Network Analysis of Dependencies of CRAN Packages*. R package version 0.0.2.

URL: <https://CRAN.R-project.org/package=crandep>

Lee, C., Garbett, A., Wang, J., Hu, B. and Jackson, D. (2019), Weaving the topics of CHI: using citation network analysis to explore emerging trends, in ‘Extended Abstracts of the 2019 CHI Conference on Human Factors in Computing Systems’.

Lee, J. (2014), Reputation computation in social networks and its applications, PhD thesis, Graduate School of Syracuse University.

Lee, J. and Oh, J. C. (2014), Estimating the degrees of neighboring nodes in online social networks, in ‘PRIMA 2014: Principles and Practice of Multi-Agent Systems’, Lecture Notes in Artificial Intelligence, Springer.

Li, H., Zhao, H., Cai, W., Xu, J. and Ai, J. (2013), ‘A modular attachment mechanism for software network evolution’, *Physica A* **392**, 2025–2037.

Louridas, P., Spinellis, D. and Vlachos, V. (2008), ‘Power laws in software’, *ACM Transactions on Software Engineering and Methodology* **18**(1).

MacDonald, A., Scarrott, C. J., Lee, D., Darlow, B., Reale, M. and Russell, G. (2011), ‘A flexible extreme value mixture model’, *Computational Statistics and Data Analysis* **55**, 2137–2157.

Mathews, P., Mitchell, L., Nguyen, G. and Bean, N. (2017), The nature and origin of heavy tails in retweet activity, in ‘Proceedings of the 26th International Conference on World Wide Web Companion’, WWW ’17 Companion, International World Wide Web Conferences Steering Committee, Republic and Canton of Geneva, Switzerland, pp. 1493–1498.

Mohd-Zaid, M. (2016), A Statistical Approach to Characterize and Detect Degradation Within the Barabasi-Albert Network, PhD thesis, Air Force Institute of Technology.

Montemurro, M. A. (2001), ‘Beyond the ZipfMandelbrot law in quantitative linguistics’, *Physica A* **300**, 567–578.

Munasinghe, R., Kossinna, P., Jayasinghe, D. and Wijeratne, D. (2019), *ptsuite: Tail Index Estimation for Power Law Distributions*. R package version 1.0.0.
URL: <https://CRAN.R-project.org/package=ptsuite>

Newman, M. E. J. (2001a), ‘Scientific collaboration networks. I. network construction and fundamental results’, *Physical Review E* **64**, 016131.

Newman, M. E. J. (2001b), ‘The structure of scientific collaboration networks’, *Proceedings of the National Academy of Sciences* **98**(2), 404–409.

Newman, M. E. J. (2004), ‘Coauthorship networks and patterns of scientific collaboration’, *Proceedings of the National Academy of Sciences* **101**, 5200–5205.

Newman, M. E. J. (2005), ‘Power laws, Pareto distributions and Zipf’s law’, *Contemporary Physics* **46**(5), 323–351.

Noh, J. D., Jeong, H.-C., Ahn, Y.-Y. and Jeong, H. (2005), ‘Growing network model for community with group structure’, *Physical Review E* **71**.

Pickands, J. (1975), ‘Statistical inference using extreme order statistics’, *The Annals of Statistics* **3**(1), 119–131.

Ramasco, J. J., Dorogovtsev, S. N. and Pastor-Satorras, R. (2004), ‘Self-organization of collaboration networks’, *Physical Review E* **70**, 036106.

Roberts, G. O. and Rosenthal, J. S. (2009), ‘Examples of adaptive MCMC’, *Journal of Computational and Graphical Statistics* **18**(2), 349–367.

Rohrbeck, C., Eastoe, E. F., Frigessi, A. and Tawn, J. A. (2018), ‘Extreme value modelling of water-related insurance claims’, *The Annals of Applied Statistics* **12**(1), 246–282.

Scarrott, C. and MacDonald, A. (2012), ‘A review of extreme value threshold estimation and uncertainty quantification’, *REVSTAT - Statistical Journal* **10**(1), 3360.

Sheridan, P. and Onodera, T. (2018), ‘A preferential attachment paradox: How preferential attachment combines with growth to produce networks with log-normal in-degree distributions’, *Scientific Reports* **8**(2811).

So, M. K. P. and Chan, R. K. S. (2014), ‘Bayesian analysis of tail asymmetry based on a threshold extreme value model’, *Computational Statistics and Data Analysis* **71**, 568–587.

Stumpf, M. P. H. and Porter, M. A. (2012), ‘Critical truths about power laws’, *Science* pp. 665–666.
URL: <https://science.sciencemag.org/content/335/6069/665>

Stumpf, M. P. H., Wiuf, C. and May, R. M. (2005), ‘Subnets of scale-free networks are not scale-free: sampling properties of networks’, *Proceedings of the National Academy of Sciences* **102**(12), 4221–4224.

Tancredi, A., Anderson, C. and O'Hagan, A. (2006), 'Accounting for threshold uncertainty in extreme value estimation', *Extremes* **9**, 87–106.

Thelwall, M. and Wilson, P. (2014), 'Regression for citation data: An evaluation of different methods', *Journal of Infometrics* **8**, 963–971.

Varga, I. (2015), Scale-free network topologies with clustering similar to online social networks, in H. Takayasu, N. Ito, I. Noda and M. Takayasu, eds, 'Proceedings of the International Conference on Social Modeling and Simulation, plus Econophysics Colloquium 2014', Spring Proceedings in Complexity, Springer, pp. 323–333.

Vázquez, A., Pastor-Satorras, R. and Vespignani, A. (2002), 'Large-scale topological and dynamical properties of the Internet', *Physical Review E* **65**.

Wan, P., Wang, T., Davis, R. A. and Resnick, S. I. (2020), 'Are extreme value estimation methods useful for network data', *Extremes* **23**, 171–195.

Wang, X. F. and Chen, G. (2003), 'Complex networks: small-world, scale-free and beyond', *IEEE Circuits and Systems Magazine* **3**(1), 6–20.

Wu, J., Holt, R. C. and Hassan, A. E. (2007), Empirical evidence for soc dynamics in software evolution, in '2007 IEEE International Conference on Software Maintenance', pp. 244–254.

Xiang, F. and Neal, P. (2014), 'Efficient MCMC for temporal epidemics via parameter reduction', *Computational Statistics and Data Analysis* **80**, 240–250.

Zhao, X., Scarrot, C., Oxley, L. and Reale, M. (2010), 'Extreme value modelling for forecasting market crisis impacts', *Applied Financial Economics* **20**, 63–72.

Zheng, X., Zeng, D., Li, H. and Wang, F. (2008), 'Analyzing open-source software systems as complex networks', *Physica A* **387**, 6190–6200.

APPENDICES

A MCMC algorithm

In this appendix, the Metropolis-within-Gibbs algorithm introduced in Section 4 is detailed. In one naive form, each component of $\boldsymbol{\theta} := (\xi_1, \xi_2, \sigma, u)$ is sampled from its conditional distribution given the other parameters. However, from trial runs it has been found that ξ_2 and σ are moderately correlated, and therefore will be sampled jointly, for the sake of efficiency. A joint sampling for ξ_1 and u is not as efficient and therefore is not applied, even though they are moderately correlated. Such inefficiency is primarily due to the discrete and multi-modality nature of u , as we have seen in the results in Section 5. The steps of the algorithm are as follows:

1. The current values in the chain are ξ_1 , ξ_2 , σ , u , and M .
2. Propose ξ_1^* from a symmetric density $q(\cdot|\xi_1)$ and accept ξ_1^* with probability $\min\left(1, \frac{\pi_M(\xi_1^*, \xi_2, \sigma, u | \mathbf{x})}{\pi_M(\xi_1, \xi_2, \sigma, u | \mathbf{x})}\right)$, as the (new) current value of ξ_1 . The ratio in the minimum function is, according to Equation 19, equivalent to $\frac{L_M(\xi_1^*, \xi_2, \sigma, u^*)\pi(\xi_1^*)\pi(u^*)}{L_M(\xi_1, \xi_2, \sigma, u)\pi(\xi_1)\pi(u)}$.
3. Propose ξ_2^* and σ^* from a symmetrical density $q(\cdot|\xi_2, \sigma)$ and accept (ξ_2^*, σ^*) jointly with probability $\min\left(1, \frac{\pi_M(\xi_1, \xi_2^*, \sigma^*, u | \mathbf{x})}{\pi_M(\xi_1, \xi_2, \sigma, u | \mathbf{x})}\right)$, as the current values of ξ_2 and σ .
4. Propose $u^* = \lfloor ue^\epsilon \rfloor$, where ϵ is from a Gaussian distribution with mean 0 and standard deviation s . Denote the CDF of the standard Gaussian distribution by Φ . Accept u^* as the current value of u with probability
$$\min\left(1, \frac{\pi_M(\xi_1, \xi_2, \sigma, u^*) \times [\Phi\left(\frac{1}{s} \log \frac{u+1}{u^*}\right) - \Phi\left(\frac{1}{s} \log \frac{u}{u^*}\right)]}{\pi_M(\xi_1, \xi_2, \sigma, u) \times [\Phi\left(\frac{1}{s} \log \frac{u^*+1}{u}\right) - \Phi\left(\frac{1}{s} \log \frac{u^*}{u}\right)]}\right).$$
5. Draw M from $\pi(M|\xi_1, \xi_2, \sigma, u, \mathbf{x})$, its conditional posterior distribution. Essentially, set M to 1 and 0 with probabilities

$$\frac{\pi_1(\xi_1, \xi_2, \sigma, u | \mathbf{x})\pi(M=1)}{\pi_1(\xi_1, \xi_2, \sigma, u | \mathbf{x})\pi(M=1) + \pi_0(\xi_1, \xi_2, \sigma, u | \mathbf{x})\pi(M=0)} \quad \text{and}$$

$$\frac{\pi_0(\xi_1, \xi_2, \sigma, u | \mathbf{x})\pi(M=0)}{\pi_1(\xi_1, \xi_2, \sigma, u | \mathbf{x})\pi(M=1) + \pi_0(\xi_1, \xi_2, \sigma, u | \mathbf{x})\pi(M=0)},$$

respectively. For steps 2 and 3, chosen to be the proposal density q are the univariate and bivariate Gaussian distributions, respectively, with mean equal to the current value of the parameter to be updated, while the proposal variance and the covariance matrix are adapted according to the procedures by Xiang and Neal (2014) and Roberts and Rosenthal (2009), respectively. A negative proposed value for the parameters with positive supports (ξ_1 , σ and u) will not cause any issue as the relevant prior at the proposed value will be 0, leading to a rejection. While this algorithm might not be the most efficient computationally or statistically, it is adequate for our applications in Section 5, due to the small number of parameters and the absence of latent variables in the mixture distributions.

B Supplementary plots

Supplementary plots are provided in this appendix. The posterior distributions of the fitted *frequencies* are calculated by multiplying that of the PMF $p_X(x)$ by the sample size. The resulting 99% credible intervals, over the whole range of data, are overlaid in Figure 13, for the version with continuity constraint. Echoing Figure 3, the fit by the version without the constraint is highly similar and is therefore not shown. The posterior density of σ is plotted in Figure 14.

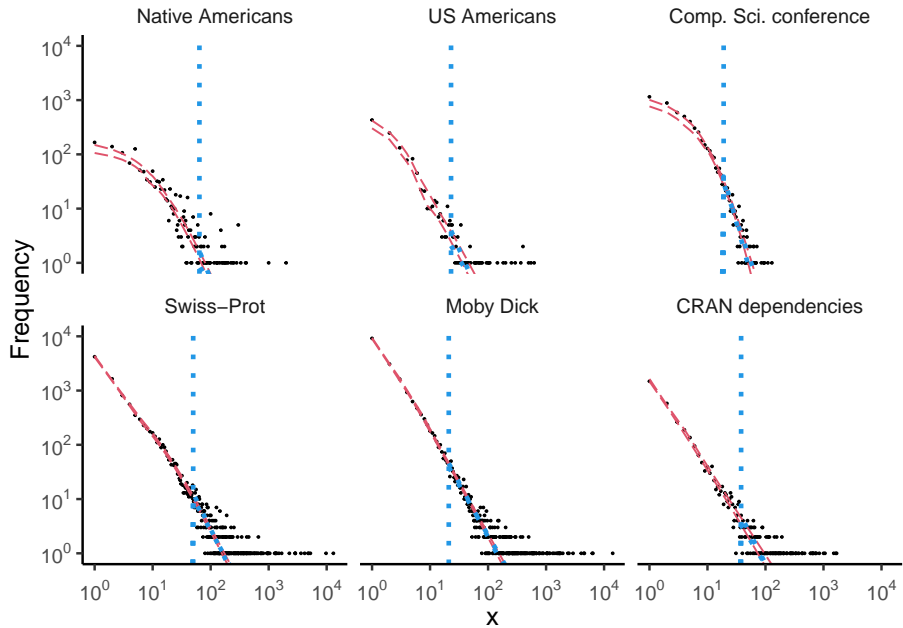


Figure 13: Frequency plots with credible intervals according to the mixture distributions with continuity constraint (red, dashed) and the discrete power law (blue, dotted) with 95% threshold (vertical).

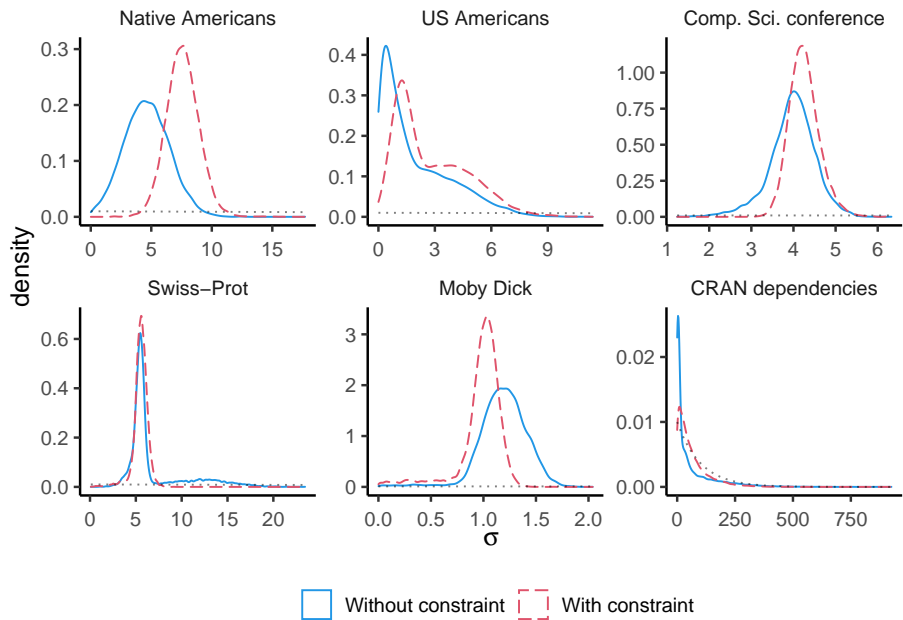


Figure 14: Prior (grey, dotted) and posterior of ϕ_u , with (red, dashed) and without (blue, solid) continuity constraint.